THE JOURNAL OF PHYSICAL CHEMISTRY B

Article

pubs.acs.org/JPCB

Effect of Nanochannel Dimension on the Transport of Water Molecules

Jiaye Su and Hongxia Guo*

Beijing National Laboratory for Molecular Sciences, Joint Laboratory of Polymer Sciences and Materials, State Key Laboratory of Polymer Physics and Chemistry, Institute of Chemistry, Chinese Academy of Sciences, Beijing 100190, China

ABSTRACT: From the perspectives of biological applications and material sciences, it is essential to understand the transport properties of water molecules through nanochannels. Although considerable effort and progress has been made in recent years, a systematic understanding of the effect of nanochannel dimension is still lacking. In this paper, we use molecular dynamics (MD) simulations to study the transport of water molecules through carbon nanotubes (CNTs) with various dimensions under pressure differences. We find an exponential decay describing the relation of the water flow and CNT lengths (L) for different pressures. The average translocation time of individual water molecules yields to a power law relation with L. We also exploit these results by comparing with the single-file transport, where some interesting relations were figured. Meanwhile, for a given CNT length, the water flow vs CNT diameters (R) can be depicted by a power law, which is found to be relevant to the water occupancy inside the nanochannel. In addition, we compare our MD results with predictions from the no-slip Hagen−Poisseuille (HP) relation. The dependence of the enhancement of the simulated water flux over the HP prediction on the CNT length and diameter supports previous MD and experimental studies. Actually, the effect of nanotube dimension is not only originated from the motion of water molecules inside the CNT but also related to thermal fluctuations in the bulk water outside the CNT. These results enrich our knowledge about the channel size effect on the water transportation, which should have deep implications for the design of nanofluidic devices.

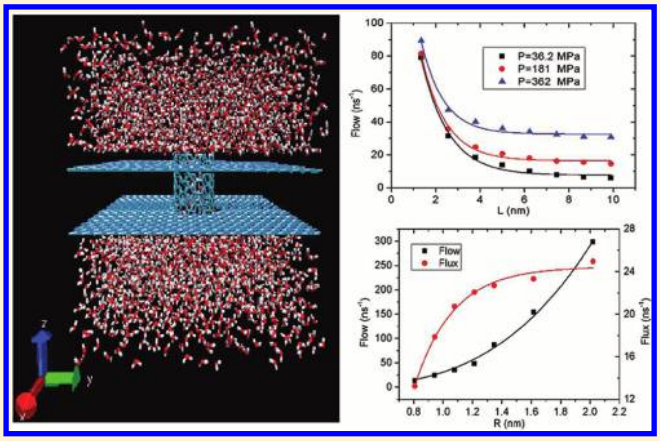

1. INTRODUCTION

Transport of fluids in narrow channels has been a subject with increasing attention in recent years due to its relevance to biological activities[1−3] and potentially industrial applications.[4−6] In fact, not only our daily life but also life itself depends on the transport of fluids through pipes, capillaries, and channels, controlled by pumps, valves, and gates.[7,8] It is known that water molecules are selectively and efficiently transported in and out of cells through the nanopores such as transmembrane proteins, aquaporins, and so on.[1,9] Unfortunately, biological water channels often contain specific and complex structures, exhibiting extraordinary transport properties that are far from being understood completely. In this sense, the study of water transportation in a structurally less complex and controllable nanofluidic modeling channel becomes a fascinating alternative, where the conditions and parameters can be conveniently tuned by experimental techniques or theoretical methods.

Carbon nanotubes (CNTs), as a prototypical one-dimensional nanomaterial, have been originally identified for their exceptional electrical, mechanical, and thermal properties. Nevertheless, subsequent experimental[10,11] and theoretical[12,13] studies proved CNTs as fast water transporters, where the water flow rate exceeds the prediction of conventional nonslip hydrodynamic flow by several orders of magnitude. Consequently, if such CNTs can be utilized in the seawater desalination or polluted water filtration, the energy required is expected to be reduced significantly. To some extent, the fast conduction of water inside CNTs is not only due to the CNT itself, such as its regular structure, its smooth interior surface, and its hydrophobic nature, but also relevant to the strong interaction between water molecules and their unique structures different from a bulk system.[3] Actually, confined water molecules can form specific clusters due to the hydrogen bonds. For example, a single-file arrangement of water molecules inside a subnanometer CNT was observed in a pioneering simulation study[12] and recent Raman spectroscopy experiments,[14] and summarized in very recent reviews.[15,16] For wider CNTs with a diameter of 1−2 nm, water molecules may form into ordered ice−tube structures under high pressure of ∼GPa.[17,18] Actually, many experiments confirm the filling of narrow CNTs with water, e.g., transmission electron microscopy,[19] nuclear magnetic resonance spectroscopy,[20] neutron diffraction,[21] and density gradient centrifugation[22] experiments. Therefore, in view of their superiority as a water transporter,

Received: December 4, 2011
Revised: March 22, 2012
Published: March 26, 2012

   dx.doi.org/10.1021/jp211650s | J. Phys. Chem. B 2012, 116, 5925−5932

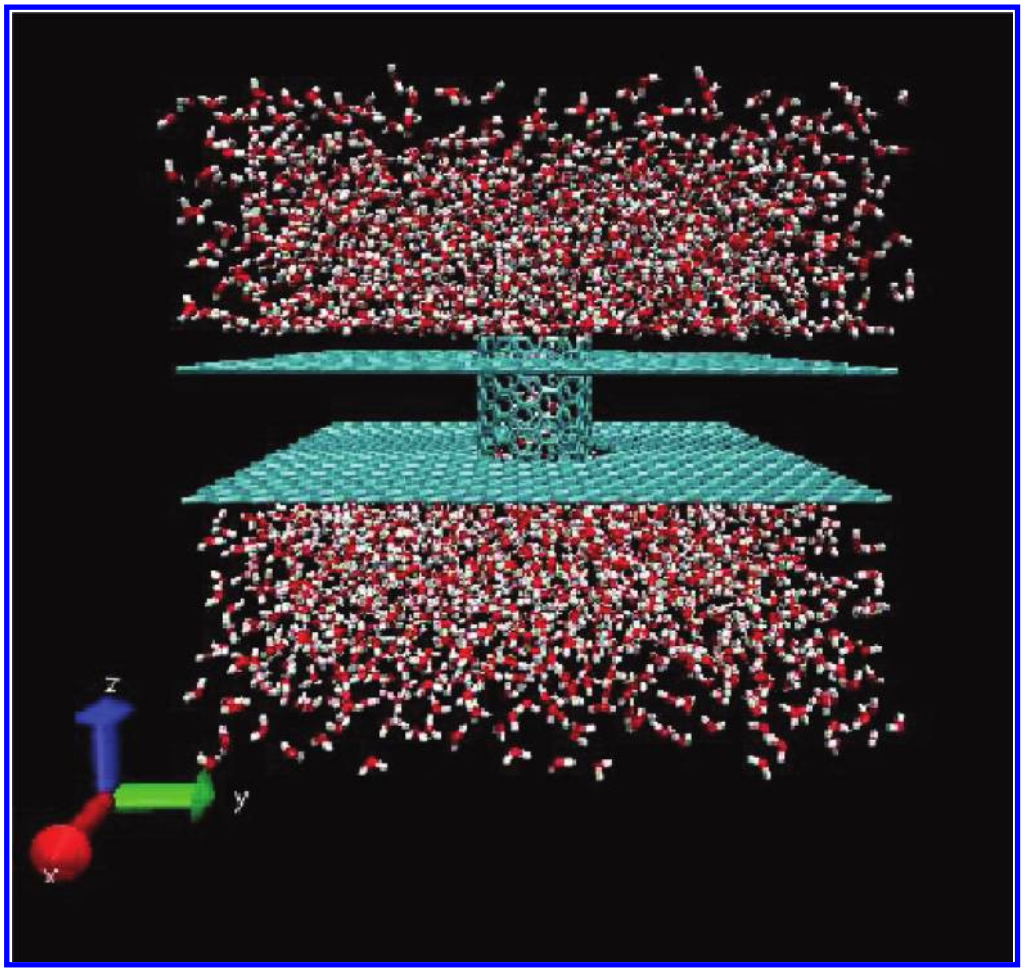

Figure 1. A snapshot of the simulation system. The (8,8) type CNT combined with two graphite sheets (5.08×5.08 nm^2) are solvated in a water box with 3136 molecules, representing a nanometer water channel. The axis of CNT is parallel to the z-axis, and an artificial pressure difference between two ends of the CNT is applied in the z-axis direction.

within the experimentally available materials, carbon nanotubes should be an ideal model of nanochannels for theoretical studies. Furthermore, it is also expected that the transport of water molecules through CNTs is also relevant to the design of novel nanofluidic devices, such as molecular sieves,[23,24] novel desalination machines,[25−27] fuel cells,[28,29] drug delivery,[30−32] biosensors,[33−35] as well as nanometer water gates.[36,37]

It has been recognized that the transport of water through CNTs is complex and often affected by many factors, such as temperatures,[20,38,39] pressures,[40] and electric fields.[38,41] In particular, not only the structures[17,18] but also the diffusion properties[42−44] and even the water flow rate[40,45] are dependent on the CNT diameter. The CNT length also has great impact on the transport properties of water molecules.[46,47] Hence, the nanochannel dimension should play an important role in the water permeation. However, the existing studies are still few and limited, and a systematic understanding about this effect is desired. On the other hand, CNTs utilized in experiments often have several nanometers in diameter and lengths up to $\sim\mu$m.[10,11] Thus, it becomes necessary for us to study the CNT-dimension effect on the transport properties of water molecules, which can aid in predicting transport behavior for large CNTs beyond our theoretical but within experimental length scales. To this end, in the present work, we use molecular dynamics (MD) simulations to systematically investigate the CNT-dimension effect on the transport properties of water molecules under various pressure differences. Interestingly, we find some scaling properties for the water flow rate, net flux, average translocation time, and water occupancy versus the CNT length or diameter. Some of these scaling forms are compared with our previous work, where we studied the CNT-length effect on the transportation of single-file water molecules in an electric field.[47] The effect of channel dimension is due to both the motion of water molecules inside the CNT and thermal fluctuations of bulk water outside the channel. The present results not only provide some new physical insights into the transport of water molecules but also demonstrate the underlying mechanism, which enrich our understanding of channel-dimension effect and are important for designing efficient nanofluidic devices.

2. MODEL AND SIMULATION METHODS

The snapshot of the simulation system in the present study is shown in Figure 1, where the CNT combined with two graphite sheets divides the water box into two equal parts. For each set of simulated systems, systematic MD simulations were performed for various values of the CNT length, diameter, and pressure difference. For a given CNT type (8,8) with 1.08 nm in diameter, we changed the CNT length from 1.34 to 9.89 nm, while, for a given CNT length of 2.56 nm, we considered a series of CNT types of (6,6), (7,7), (8,8), (9,9), (10,10), (12,12), and (15,15), corresponding to diameters of 0.81, 0.94,

dx.doi.org/10.1021/jp211650s | J. Phys. Chem. B 2012, 116, 5925−5932

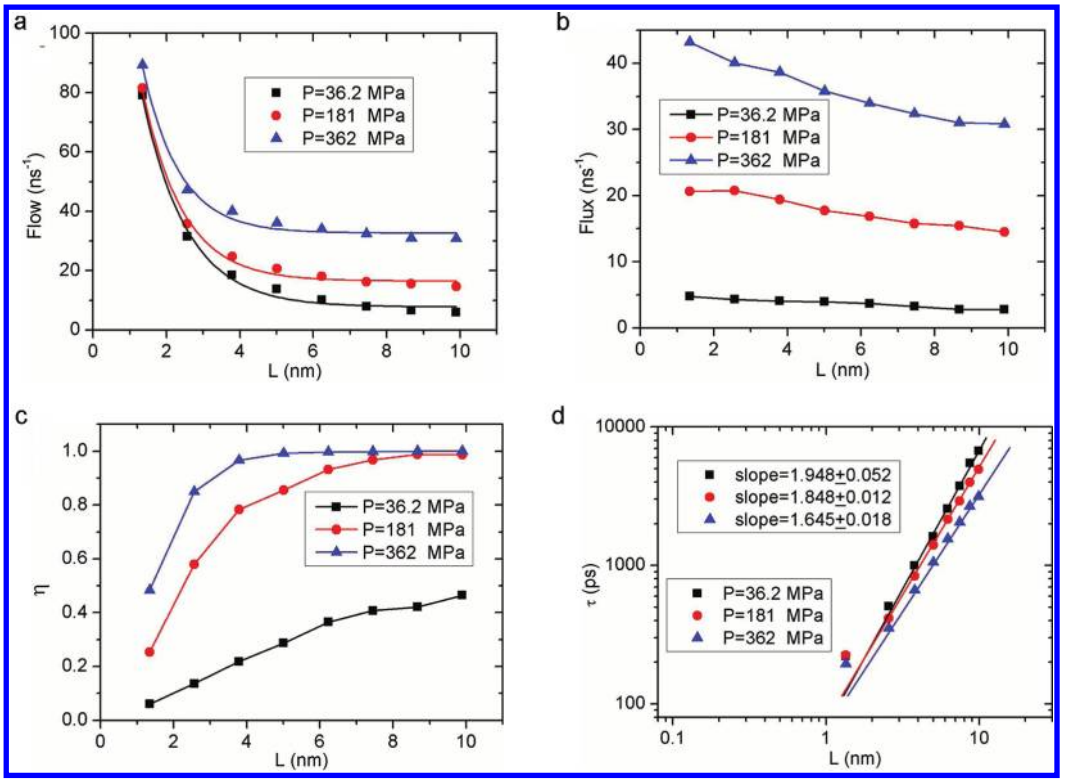

Figure 2. (a) Water flow, (b) water flux, (c) unidirectional transport efficiency η, and (d) average translocation time τ of individual water molecules as a function of CNT lengths under pressure of P = 36.2, 181, and 362 MPa. The data in part a are fitted by same color lines according to the function of $f_W(L) = A_0 \exp(-L/L_0) + f_{W0}$. The data in part d are fitted by same color lines linearly except for the first points.

1.08, 1.21, 1.35, 1.62, and 2.02 nm, respectively. The number of water molecules in each setup system is fixed to 3136. Throughout, the x and y dimensions of the simulation box are held at the same value of 5.08 nm, but the z dimension varies depending on CNT lengths. The center of the CNT was set as the center of the whole simulation box. For convenience, we assumed the CNT center at the position of x = 0 nm, y = 0 nm, and z = 0 nm. The axis of the CNT is parallel to the z-axis and a pressure difference between the two ends of the CNT is also applied in the z direction. Following the method proposed by Zhu et al.,[48] we applied the additional acceleration of 0.01, 0.05, and 0.1 nm/ps^2 to each water molecule along the $+z$ direction to obtain pressure differences of about 36.2, 181, and 362 MPa between the two ends of the CNT, respectively. We define the upflux/downflux as the total number of water molecules per nanosecond conducted through the CNT from bottom/top ($-z/+z$) to top/bottom ($+z/-z$), respectively. The flow is the sum of upflux and downflux, while the flux is the difference between them.[12,15,41,46,47]

All MD simulations were carried out at constant volume and temperature (300 K) using the Nose–Hoover method for temperature coupling with the Gromacs 3.3.1 package.[49] The TIP3P water model was used.[50] The carbon atoms were modeled as uncharged Lennard-Jones particles, and the carbon–carbon and carbon–water interaction parameters were taken from Hummer et al.[12] The particle-mesh Ewald method[51] was used to treat the long-range electrostatic interactions. Periodic conditions were applied in all directions. During the simulations, the carbon nanotubes combined with two graphite sheets were held fixed. A time-step of 2 fs was used, and data were collected every 0.5 ps. We conducted 130 ns MD runs for each set of systems, and the trajectories of the last 120 ns were used for data analysis. The total simulation time was up to ~3.9 μs, which was still time-consuming for the current atomic system of ~12000 atoms.

3. RESULTS AND DISCUSSION

In a previous simulation study, we discussed the effect of CNT length on the transportation of single-file water molecules in electric fields.[47] Although single-file water chains have attracted broad theoretical interest due to their unique dynamics,[15,16] from a technique point of view, it is difficult to design CNTs with a diameter as small as only allowing for the single-file arrangement,[14] and generally the wider CNTs with diameters of several nanometers serve as water transporters,[10,11] wherein water molecules are not in a single-file structure. Also, compared with the electric field, applying an external pressure gradient is a more realistic and effective method to transport water directionally in experiments.[10,11] Thus, in the present study, we use CNT (8,8) with a diameter of 1.08 nm as the main system to investigate the CNT-length effect, and apply the pressure difference as the driving force. The (8,8) type CNT can accommodate three water molecules at the radial plane, which can typically represent a non-single-file water arrangement. As shown in Figure 2, the transport properties of water molecules through (8,8) CNTs under different pressures are described as a function of CNT lengths.

The decay of water flow with increasing CNT length (L) in Figure 2a shows similar behavior for different pressures. Remarkably, as the CNT length increases, the water flow decreases exponentially, since water molecules need more time to travel through longer CNTs. Interestingly, as seen for the fitted lines, the water flow can be well described by the function of $f_W(L) = A_0 \exp(-L/L_0) + f_{W0}$, where A_0, L_0, and f_{W0} are

dx.doi.org/10.1021/jp211650s | J. Phys. Chem. B 2012, 116, 5925–5932

constant, and dependent on pressures. For P = 36.2, 181, and 362 MPa, A_0 = 215, 223, and 217 ns^{-1}, L_0 = 1.21, 1.09, and 1.0 nm, and f_{W0} = 7.75, 16.46, and 32.64 ns^{-1}, respectively. Clearly, f_{W0} represents the asymptotic value of water flow at the infinite length of CNTs, which is strongly dependent on pressures. It should be noted that the present study refers to non-single-file transport, where water molecules inside the CNT channel can slip with each other. For the single-file transport,[15,16] the motion of water molecules inside the CNT is highly collective, and they cannot slip with each other. This difference should have a profound impact on their transport properties.

In a previous study, Berezhkovskii and Hummer[52] proposed a continuous-time random walk (CTRW) model to describe the single-file transport, where they predicted a power law decay ($\sim 1/L$) for the water flow in the free case. Subsequently, Li et al.[53] found a faster power low decay ($\sim L^{-2.3}$) by the use of MD simulations, which was confirmed by our previous study.[47] Besides, we also suggested an exponential decay of $\sim\exp(-L/L_0)$ for longer CNTs. It seems that the exponential decay of water flow of $\sim\exp(-L/L_0)$ is independent of pressure differences and electric field strengths. Also, whether for the single-file water chain or for the non-single-file structure in the present study, the decay relation does not alter. That is to say, such a decay is intrinsic for the water flow through CNTs, which should be less sensitive to diameter or external fields. However, the magnitudes of constants A_0, L_0, and f_{W0} are always affected by external factors. For different electric field strengths, these values are close to each other,[47] as the electric field does not exert any additional force on water molecules. An interesting phenomenon is that the value of L_0 under pressures is about twice of those in electric fields,[47] where the difference is expected to be relevant to CNT diameters or the resultant different water arrangements (single-file vs non-single-file), rather than the different working principles between pressure and electric field. Similar to our previous analysis,[47] if we use the reduced length $L_R^* = L/0.26$ (0.26 nm is the unit length of CNTs), we furthermore obtain a scaling function of $f_W(L) \sim \exp(-L_R^*/4)$, compared to the scaling of $\sim\exp(-L_R^*/2)$ for the single-file transport in electric fields. However, owing to the complex water arrangement in the non-single-file water transportation, we cannot include the H-bond demonstration further as we did for the single-file transport in electric fields. It is not surprising that the water flow shows a slower decay for the present non-single-file transport, where water molecules inside the CNT can slip with each and thus they enter one end of the CNT and leave the other end quickly. For example, for L = 5.0 nm, the water flows are 17.4 and 6.6% of those for L = 1.34 nm, for P = 36.2 MPa and E = 0.1 V/nm,[47] respectively.

Figure 2b shows the dependence of net water flux on the CNT length for different pressures. It is clear that for a given CNT length the flux is proportional to the pressure, in agreement with the Hagen−Poiseuille relation and MD results.[40] As a whole, the water flux decreases as the CNT length increases. However, the decrease rate is reduced for longer CNTs, and this trend is more obvious for larger pressures. For example, at P = 362 MPa, for the same increase of L = 1.34−2.56, 5.01−6.23, and 8.67−9.89 nm, the decrease of flux is 3.12, 1.82, and 0.21 ns^{-1}, respectively. For the same L and P, the water flux is always smaller than the water flow. These results should be relevant to the competition between the pressure-driven motion of water molecules inside the CNT channel and the thermal fluctuation of bulk water outside the CNT channel. For short CNTs, the distance between water molecules inside CNTs and those in the two reservoirs is short, and thus the motion of inside water molecules can be highly affected by thermal fluctuations of reservoirs. Even under the drive of a large pressure difference, a large amount of water molecules can still move against the pressure gradient direction. For instance, the flux and flow are 43.18 and 89.33 ns^{-1}, respectively, for L = 1.34 nm and P = 362 MPa, that is to say there are 23.08 (about a quarter of total flow) water molecules transporting through the CNT against the pressure per nanosecond. For long CNTs, the distance becomes long, and the motion of water molecules inside the CNT is less sensitive to reservoirs. The portion of water flow against the pressure direction also is reduced. To quantitatively describe this effect, we introduce the unidirectional transport efficiency η defined as flux/flow.[47] Clearly, the range of η is 0−1, and η = 0 represents water molecules transport equally in the $\pm z$ direction, where the pressure should be zero; η = 1 denotes water molecules transporting completely along the pressure direction.

The unidirectional transport efficiency is shown as a function of CNT lengths for different pressures in Figure 2c. Remarkably, η increases with L, implying that the pressure becomes more dominant than the thermal fluctuation effect of reservoirs. For $L \geq$ 5.01 nm, η is above 0.99 for P = 362 MPa, where water molecules transport against the pressure gradient direction rarely. Unlike the electric field,[47] the pressure has a great impact on η. For a given L, higher η is observed for the larger pressure, since the larger driving force can well overcome thermal fluctuations of reservoirs. For example, η = 0.287, 0.855, and 0.992 for L = 5.01 nm and P = 36.2, 181, and 362 MPa, respectively. These results indicate that the choice of some controlling parameters, such as CNT length and pressure here, is the key to achieve unidirectional water transportation, which should have deep implications for the design of efficient nanofluidic devices for use in desalination,[25−27] drug delivery,[30−32] and so on. In hope of transporting drugs in a desired direction by a water flow, we should reduce or eliminate the partial flow against that direction so as to increase efficiency.

In order to further understand the effect of CNT length on the transport dynamics, we calculated the average translocation time of individual water molecules, presented in Figure 2d. Clearly, a power law scaling $\tau \sim L^{\upsilon}$ describes the relation of τ vs L. Note that the first data of L = 1.34 nm are ignored in the fitting due to the intense influence of reservoirs. The value of υ decreases with the increase of pressure, as larger pressures will lead to shorter translocation times. In a previous study, Striolo[42] showed that, for the same CNT diameter (R = 1.08 nm), water molecules diffuse through a fast ballistic motion ($dr^2 \sim dt^2$, where dr^2 is the mean-square distance) mechanism for up to 500 ps, and then transfer to Fickian-type diffusion ($dr^2 \sim dt$) for long times. For the Fickian-type diffusion in one dimension (i.e., along the z direction), one has $\langle \Delta z^2 \rangle = 2Dt$; thus, $t \sim L^2$ can be expected. For the low pressure of P = 36.2 MPa, we obtained $\upsilon = 1.948 \pm 0.052$, which is very close to the diffusion exponent of 2. This agreement is rational, as under weak pressures, the case should be close to the self-diffusion process.

It will be more interesting to compare the current results with the single-file transport. In electric fields,[47] the translocation time exhibits similar power law scaling of $\tau \sim L^{\upsilon}$ with larger υ of 2.742−2.970. The difference should be due to the CNT diameter or the structure of water molecules. For the single-file transport, the motion of water molecules is highly

collective,[15,16] and they cannot slip with each other as in the non-single-file transport. Hence, it should take a longer time for individual water molecules to travel though the CNT channel, leading to a larger value of υ. For L = 5.0 nm, the translocation times are 10.34 and 1.61 ns for E = 0.1 V/nm and P = 36.2 MPa, respectively. On the other hand, Mukherjee et al.[44] showed that the single-file water chain exhibits Fickian diffusion; however, when more than one single-file water chain exists or the entire chain breaks down to two or more parts, single-file diffusion (SFD, where $dr^2 \sim dt^{1/2}$) is observed. Thus, the observed υ of 2.742−2.970 for the single-file transport can be well understood, as the single-file water chain inside the CNT channel does not always keep entirely from the fluctuating water occupancy. In a word, without any driving force, the difference of υ between the single-file and the non-single-file transportations clearly exists, and the ratio is about 3/2 (take P = 36.2 MPa and E = 0.1 V/nm as a comparison).

Until now, we have discussed the effect of CNT length on the transport dynamics of non-single-file water molecules under pressure differences. In the following, we will further discuss the effect of CNT diameters. We give the water flow and flux in Figure 3a as a function of CNT diameter R for P = 181 MPa.

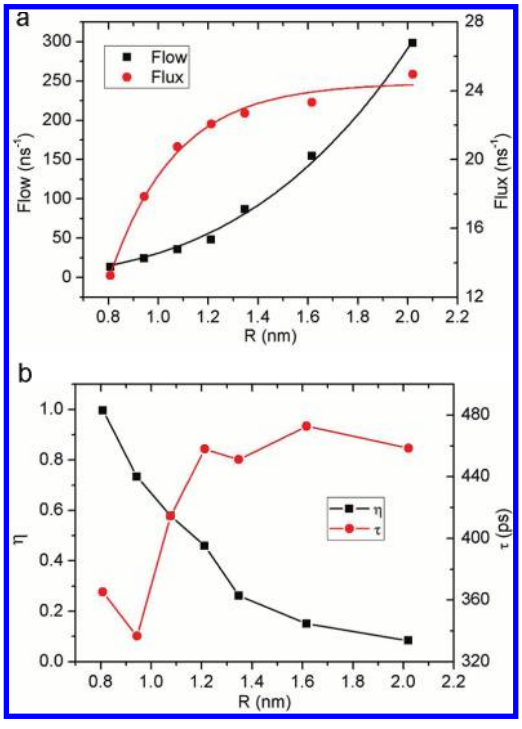

Figure 3. (a) Water flow and flux and (b) unidirectional transport efficiency η and average translocation time τ of individual water molecules as a function of CNT diameters under a pressure of P = 181 MPa. Data of flow and flux are fitted by same color lines according to the function of $f_W(R) = B_0R^{\mu}$ and $f_X(R) = -C_0 \exp(-R/R_0) + f_{X0}$, respectively.

The water flow increases dramatically with R, which can be well fitted as a power law of $f_W(R) \sim R^{\mu}$ with μ = 3.230, shown for the same color line. Considering the fact that, for larger diameters, more water molecules at the channel inlet/outlet are exposed to water reservoirs, wider CNTs have more opportunity to generate water flow. Therefore, $f_W(R) \sim \langle N\rangle/L$ is expected, where $\langle N\rangle \sim V$ is the average water occupancy and $V \sim LR^2$ is the channel volume. In fact, from the numerical simulation, we will show in the following that $\langle N\rangle \sim R^{\kappa}$ with $\kappa > 2$ is obtained due to specific water structures forming inside narrow channels. For the water flux also shown in Figure 3a, we can see that it increases with R, where the increase rate becomes lower. According to this trend, we fit the data into the function of $f_X(R) = -C_0 \exp(-R/R_0) + f_{X0}$, where C_0 = 236 ns^{-1}, R_0 = 0.26 nm, and f_{X0} = 24.45 ns^{-1}. As the increase of R, more water molecules inside the CNT can be affected by thermal fluctuations of reservoirs. The increase of water molecules moving along the pressure direction will be associated with the increase on the opposite direction, leading to the slower increase of flux for larger R. For example, for R = 1.08, 1.35, and 2.02 nm, the number of water molecules along and opposite the pressure gradient is 3396, 6559, and 19399 and 906, 3835, and 16404, respectively. Hence, there should be a competition between the pressure and the thermal fluctuation of reservoirs.

The unidirectional transport efficiency η shown in Figure 3b further confirms such a competition. For R = 0.81 nm, i.e., the case of single-file transport, we obtain η > 0.99, where only three water molecules are conducting against the pressure and 1594 along. As the increase of R, η decreases remarkably, and to about 0.08 for the largest R = 2.02 nm. The average translocation time of individual water molecules also displayed in Figure 3b does not follow the aforementioned scaling behavior. As a whole, τ increases slightly and to saturation with the increase of R, which should stem from the competition between the pressure driven transportation and the thermal fluctuation from reservoirs. As we discussed above, for a given CNT length (referring to relatively longer CNTs), the translocation time should be larger for the single-file transport.

We further calculated the average water occupancy inside the CNT channel, and the results are given in Figure 4. For the

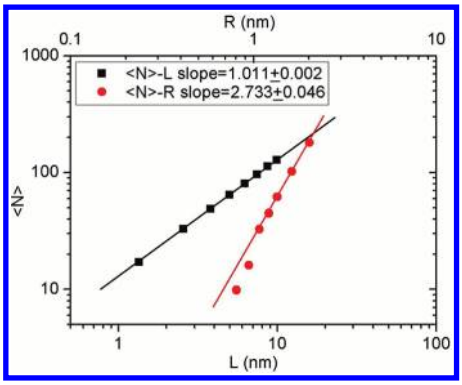

Figure 4. Average occupancy of water molecules inside the CNT as a function of CNT lengths and diameters, respectively, under a pressure of P = 181 MPa. Both of them are fitted linearly by same color lines except for the first two points of diameter data.

given CNT diameter of R = 1.08 nm, $\langle N\rangle$ increases linearly with L, which is in agreement with the single-file case.[47] As we mentioned above, $\langle N\rangle$ should be proportional to the channel volume, i.e., $\langle N\rangle \sim LR^2$. However, a lager power law ($\langle N\rangle \sim R^{\kappa}$) exponent κ = 2.733 is obtained from our numerical simulation. This result should be relevant to the unique ordered water structure inside narrow CNT channels.[12,17,18] For diameters around ∼1 nm, water molecules will form single-file or ice-tube structures, which may occupy a smaller volume, leading to a larger exponent. Note that in the fitting process we ignored the first two data (R = 0.81, 0.94 nm), as the two

dx.doi.org/10.1021/jp211650s | J. Phys. Chem. B 2012, 116, 5925−5932

deviate the others slightly, where water molecules form single-file and double-file, respectively. In fact, if we include the two data, an even larger exponent $\kappa = 3.196 \pm 0.177$ can be obtained. Thus, the above assumption of $f_W(R) \sim \langle N \rangle / L \sim R^\kappa$, is very close to the numerical result of $f_W(R) \sim R^\mu$, where $\mu = 3.230$. To some extent, this accordance validates our assumption of water flow.

In order to further understand the effect of channel dimension on the water occupancy or the dynamics of fill-empty,[12] we calculated the probability distribution of water occupancy, shown in Figure 5. For a given diameter of $R = 1.08$ nm, the occupancy distribution becomes wider with lower peak values as the increase of L. For example, the width of $L = 2.56$ nm is 16 ($N = 24-40$), and it increases to 26 ($N = 114-140$) for $L = 9.89$ nm. A similar trend is observed when we vary the diameter for a given length. Actually, it should be easy for water molecules to arrange themselves to accommodate larger confinement, which can bear higher fluctuations of water occupancy; while for smaller confinement, due to the exclude volume effect from the Lennard-Jones potentials and the strong interactions of hydrogen bonds, high occupancy fluctuations are forbidden. Hummer et al. showed that a small change of water−CNT interaction can lead to the occupancy fluctuation remarkably.[12]

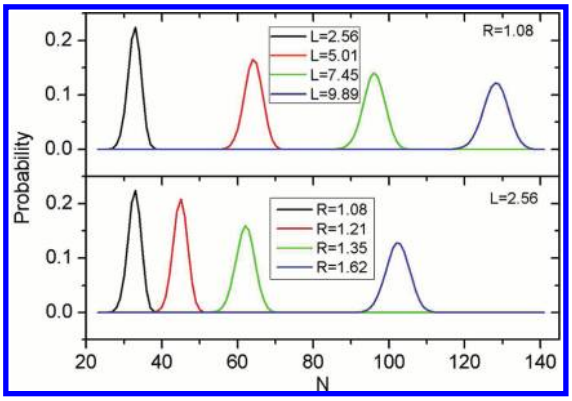

Figure 5. Probability distribution of water occupancy inside CNTs with different dimensions under a pressure of $P = 181$ MPa.

In previous studies,[40,45] Thomas and McGaughey found that the water flow rate is strongly dependent on CNT diameters. They made a deep comparison for the MD results with those predicted by the Hagen−Poisseuille law, and the enhancement (the ratio of MD flux to the prediction of no-slip Hagen−Poisseuille Q_N) was found to be decreasing with the increase of CNT diameters, where the value is remarkably lower than previous experimental presentations.[10,11] To further understand the effect of CNT dimension on the water transportation, we also calculated the enhancement for different CNT lengths and diameters, shown in Figure 6a. According to previous studies,[11,40] the water flux of no-slip Hagen−Poisseuille can be $Q_N = \pi(d/2)^4 \Delta P / 8\lambda L$, where d is the effective diameter of CNT channels, ΔP is the pressure difference, and λ is the water viscosity. When calculating Q_N, the effective diameter $d = R - 2\delta_{CO}$, where $\delta_{CO} = 0.3275$ nm is the carbon−water Lennard-Jones radius, and the experimental value of water viscosity, 0.89 mPa,[40] were used.

It is clear from Figure 6a that, for a given CNT length $L = 2.56$ nm, the enhancement reduces immediately as the CNT diameter increases, which is in agreement with the previous

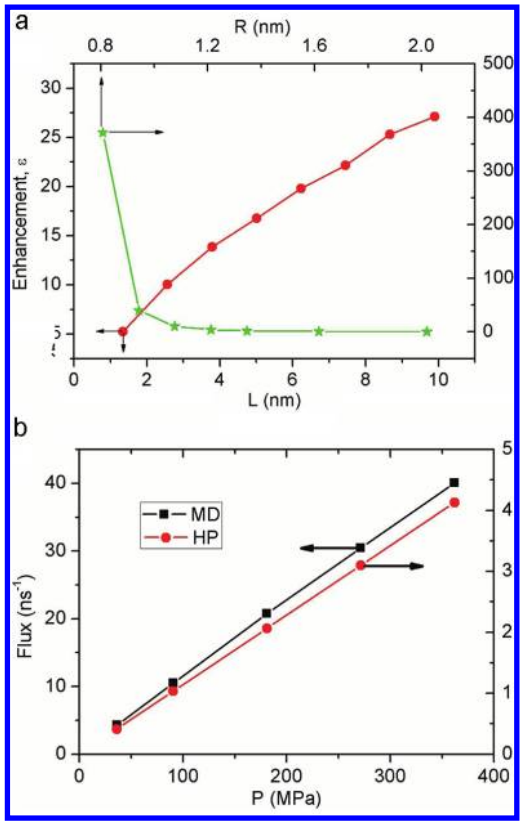

Figure 6. (a) Enhancement (calculated flux divided by Q_N, where Q_N is the flux predicted by the no-slip Hagen−Poisseuille relation) of MD results as a function of the CNT length L ($R = 1.08$ nm) and diameter R ($L = 2.56$ nm), under $P = 181$ MPa. (b) Water flux as a function of pressure for MD simulations and the prediction of the no-slip Hagen−Poisseuille relation, for a given CNT with $L = 2.56$ nm and $R = 1.08$ nm.

study.[40] For $R = 1.08$ nm, the enhancement increases almost linearly with L. In Figure 6b, for different pressures, the MD water flux is only an order larger than Q_N. As a whole, similar to the simulation study,[40] the enhancement is lower than the experimental reports.[10,11] Nevertheless, the experimental CNT length was up to ~μm, while the CNT length in the present and previous[40] studies is only ~10 nm. Subsequent MD study by Thomas and McGaughey confirmed that the CNT length indeed has a significant impact on the enhancement.[45] For the same diameter CNT, the enhancement can be increased from 1−10 to 100−1000, when the CNT length increases from 1.3/2.6 to 75/150 nm. Therefore, both the low enhancement in the present and previous studies[40] and the high enhancement estimated by experiments[10,11] should be rational.

Finally, it should be noted that the Hagen−Poisseuille law describes laminar macroscopic fluids, and thus it remains questionable if it can be suitable for the current nanoscale channels. Although as shown in Figure 6b the linear relation of water flux with pressure gradient predicted by the no-slip Hagen−Poisseuille relation can be reproduced by MD results, the power law scalings of $Q_N \sim d^4$ and $Q_N \sim 1/L$ are different from MD results. One may relate the water flow in Figure 3a to the no-slip Hagen−Poisseuille relation, since the water flow scales as $f_W(R) \sim R^\mu$, where $\mu = 3.230$. We also should point out that, according to our definition, the water flow in our present study does not have direction, while the net water flux is induced by pressure gradients. Thus, all the comparisons with

dx.doi.org/10.1021/jp211650s | J. Phys. Chem. B 2012, 116, 5925−5932

the no-slip Hagen−Poisseuille relation should be water flux, where the disagreement may stem from the length-scale mismatch.

4. CONCLUSION

In summary, we have systematically investigated the effect of nanochannel dimension on the transport of water molecules under the drive of pressures. For a given channel diameter and a non-single-file water arrangement, we find that the water flow vs CNT lengths follows an exponential decay of $f_W(L) \sim \exp(-L/L_0)$ for different pressures, which is similar to our previous study of single-file transport.[47] The water flux decreases as L increases, and is strongly dependent on pressures. The unidirectional transport efficiency η increases with L. The average translocation time of individual water molecules yields to a power law of $\tau \sim L^{\upsilon}$, where υ slightly depends on the pressures. When comparing with the single-file case, we find that the value of υ is sensitive to the water structures.

Meanwhile, for a given CNT length, the water flow and flux vs CNT radius (R) can be depicted by a power law of $f_W(R) \sim R^{\mu}$ and an exponential relation of $f_X(R) \sim -\exp(-R/R_0)$, respectively. The unidirectional transport efficiency η decreases with increasing R. The water occupancy inside the CNT shows the relation of $\langle N \rangle \sim L$ and $\langle N \rangle \sim R^{\kappa}$. Actually, the water flow should be relevant to water molecules at the inlet/outlet of the CNT that are exposed to reservoirs. Interestingly, if we assume $f_W(R) \sim \langle N \rangle / L$, a similar relation of $f_W(R) \sim R^{\kappa}$ can be obtained, where κ is close to μ. The distribution of water occupancy becomes wider with low peak value as the increase of L or R.

We also compared our MD results with the prediction of the no-slip Hagen−Poisseuille relation. For a given CNT length, the enhancement decreases with the increase of CNT diameter, while, for a given CNT diameter, the enhancement increases with CNT length almost linearly. These results are in agreement with previous MD studies,[40,45] and also support previous experimental reports.[10,11] In consequence, the enhancement is strongly dependent on the nanochannel dimension.

These results stem from the competition between the pressure driven transportation and the thermal fluctuation from reservoirs, which not only enrich our knowledge about the channel size effect on the water transportation but should also have deep implications for the design of nanofluidic devices, such as desalination, drug delivery, and so on. For example, if we want to transport water-soluble ions or drugs through a fluidic nanochannel, we should tune some controlling parameters, such as the pressure, the channel diameter, or length here, so as to reduce or eliminate opposite water flow and increase efficiency. Although, due to our computational ability, the length scale of the channel we studied is still limited to ∼10 nm, some scaling behaviors for the water flow, flux, translocation time, or water occupancy are well established, which should be helpful for predicting the transport properties of water molecules when the channel size is up to experimental scales of ∼μm.

AUTHOR INFORMATION

Corresponding Author

*E-mail: hxguo@iccas.ac.cn.

Notes

The authors declare no competing financial interest.

ACKNOWLEDGMENTS

This work is financially supported by Chinese Academy of Sciences (KJCX2-YW-H19) and NSF China (20874110). The allocated computer time at the Supercomputer Center of Chinese Academy of Sciences is gratefully acknowledged.

REFERENCES

(1) De Groot, B. L.; Grubmuller, H. *Science* **2001**, *294*, 2353−2537.
(2) Ball, P. *Chem. Rev.* **2008**, *108*, 74−108.
(3) Rasaiah, J. C.; Garde, S.; Hummer, G. *Annu. Rev. Phys. Chem.* **2008**, *59*, 713−740.
(4) Furukawa, H.; Ko, N.; Go, Y. B.; Aratani, N.; Choi, S. B.; Choi, E.; Yazaydin, A. O.; Snurr, R. Q.; O'Keeffe, M.; Kim, J.; Yaghi, O. M. *Science* **2010**, *329*, 424−428.
(5) Zhou, W. Y.; Bai, X. D.; Wang, E. G.; Xie, S. S. *Adv. Mater.* **2009**, *21*, 4565−4583.
(6) Rosi, N. L.; Eckert, J.; Eddaoudi, M.; Vodak, D. T.; Kim, J.; O'Keeffe, M.; Yaghi, O. M. *Science* **2003**, *300*, 1127−1129.
(7) Tyree, M. T. *Nature* **2003**, *423*, 923−923.
(8) Ku, D. N. *Annu. Rev. Fluid Mech.* **1997**, *29*, 399−434.
(9) Agre, P. *Angew. Chem., Int. Ed.* **2004**, *43*, 4278−4290.
(10) Majumder, M.; Chopra, N.; Andrews, R.; Hinds, B. *Nature* **2005**, *438*, 44−44.
(11) Holt, J. K.; Park, H. G.; Wang, Y.; Stadermann, M.; Artyukhin, A. B.; Grigoropoulos, C. P.; Noy, A.; Bakajin, O. *Science* **2006**, *312*, 1034−1037.
(12) Hummer, G.; Rasaiah, J. C.; Noworyta, J. P. *Nature* **2001**, *414*, 188−190.
(13) Joseph, S.; Aluru, N. R. *Nano Lett.* **2008**, *8*, 452−458.
(14) Cambré, S.; Schoeters, B.; Luyckx, S.; Goovaerts, E.; Wenseleers, W. *Phys. Rev. Lett.* **2010**, *104*, 207401.
(15) Fang, H. P.; Wan, R. Z.; Gong, X. J.; Lu, H. J.; Li, S. Y. *J. Phys. D: Appl. Phys.* **2008**, *41*, 103002.
(16) Kofinger, J.; Hummer, G.; Dellago, C. *Phys. Chem. Chem. Phys.* **2011**, *13*, 15403−15417.
(17) Koga, K.; Gao, G. T.; Tanaka, H.; Zeng, X. C. *Nature* **2001**, *412*, 802−805.
(18) Bai, J. E.; Wang, J.; Zeng, X. C. *Proc. Natl. Acad. Sci. U.S.A.* **2006**, *103*, 19664−19667.
(19) Naguib, N.; Ye, H.; Gogotsi, Y.; Yazicioglu, A. G.; Megaridis, C. M.; Yoshimura, M. *Nano Lett.* **2004**, *4*, 2237−2243.
(20) Wang, H. J.; Xi, X. K.; Kleinhammes, A.; Wu, Y. *Science* **2008**, *322*, 80−83.
(21) Kolesnikov, A. I.; Zanotti, J.-M.; Loong, C.-K.; Thiyagarajan, P.; Moravsky, A. P.; Loutfy, R. O.; Burnham, C. J. *Phys. Rev. Lett.* **2004**, *93*, 035503.
(22) Cambré, S.; Wenseleers, W. *Angew. Chem., Int. Ed.* **2011**, *50*, 2764−2768.
(23) Sholl, D. S.; Johnson, J. K. *Science* **2006**, *312*, 1003−1004.
(24) Li, N.; Wang, X. M.; Derrouiche, S.; Haller, G. L.; Pfefferle, L. D. *ACS Nano* **2010**, *4*, 1759−1767.
(25) Kalra, A.; Garde, S.; Hummer, G. *Proc. Natl. Acad. Sci. U.S.A.* **2003**, *100*, 10175−10180.
(26) Service, R. F. *Science* **2006**, *313*, 1088−1090.
(27) Corry, B. *J. Phys. Chem. B* **2008**, *112*, 1427−1434.
(28) Yuan, Q. Z.; Zhao, Y. P. *J. Am. Chem. Soc.* **2009**, *131*, 6374−6376.
(29) Zhao, Y. C.; Song, L.; Deng, K. *Adv. Mater.* **2008**, *20*, 1772−1776.
(30) Bhirde, A. A.; Patel, V.; Gavard, J.; Zhang, G. F.; Sousa, A. A.; Masedunskas, A.; Leapman, R. D.; Weigert, R.; Gutkind, J. S.; Rusling, J. F. *ACS Nano* **2009**, *3*, 307−316.
(31) Bianco, A.; Kostarelos, K.; Prato, M. *Curr. Opin. Chem. Biol.* **2005**, *9*, 674−679.

(32) Liu, Z.; Sun, X. M.; Nakayama-Ratchford, N.; Dai, H. J. *ACS Nano* **2007**, *1*, 50−56.
(33) Javey, A. *ACS Nano* **2008**, *2*, 1329−1335.
(34) Tu, Y. S.; Xiu, P.; Wan, R. Z.; Hu, J.; Zhou, R. H.; Fang, H. P. *Proc. Natl. Acad. Sci. U.S.A.* **2009**, *106*, 18120−18124.
(35) Ghosh, S.; Sood, A. K.; Kumar, N. *Science* **2003**, *299*, 1042−1044.
(36) Li, J. Y.; Gong, X. J.; Lu, H. J.; Li, D.; Fang, H. P.; Zhou, R. H. *Proc. Natl. Acad. Sci. U.S.A.* **2007**, *104*, 3687−3692.
(37) Wan, R. Z.; Li, J. Y.; Lu, H. J.; Fang, H. P. *J. Am. Chem. Soc.* **2005**, *127*, 7166−7170.
(38) Vaitheeswaran, S.; Rasaiah, J. C.; Hummer, G. *J. Chem. Phys.* **2004**, *121*, 7955−7964.
(39) Zambrano, H. A.; Walther, J. H.; Koumoutsakos, P.; Sbalzarini, I. F. *Nano Lett.* **2009**, *9*, 66−71.
(40) Thomas, J. A.; McGaughey, A. J. H. *Nano Lett.* **2008**, *8*, 2788−2793.
(41) Su, J. Y.; Guo, H. X. *ACS Nano* **2011**, *5*, 351−359.
(42) Striolo, A. *Nano Lett.* **2006**, *6*, 633−639.
(43) Mashl, R. J.; Joseph, S.; Aluru, N. R.; Jakobsson, E. *Nano Lett.* **2003**, *3*, 589−592.
(44) Mukherjee, B.; Maiti, P. K.; Dasgupta, C.; Sood, A. K. *ACS Nano* **2010**, *4*, 985−991.
(45) Thomas, J. A.; McGaughey, A. J. H. *Phys. Rev. Lett.* **2009**, *102*, 184502.
(46) Wan, R. Z.; Lu, H. J.; Li, J. Y.; Bao, J. D.; Hu, J.; Fang, H. P. *Phys. Chem. Chem. Phys.* **2009**, *11*, 9898−9902.
(47) Su, J. Y.; Guo, H. X. *J. Chem. Phys.* **2011**, *134*, 244513.
(48) Zhu, F. Q.; Tajkhorshid, E.; Schulten, K. *Biophys. J.* **2002**, *83*, 154−160.
(49) Lindahl, E.; Hess, B.; van der Spoel, D. *J. Mol. Model.* **2001**, *7*, 306−317.
(50) Jorgensen, W. L.; Chandrasekhar, J.; Madura, J. D.; Impey, R. W.; Klein, M. L. *J. Chem. Phys.* **1983**, *79*, 926−935.
(51) Essmann, U.; Perera, L.; Berkowitz, M. L.; Darden, T.; Lee, H.; Pedersen, L. G. *J. Chem. Phys.* **1995**, *103*, 8577−8593.
(52) Berezhkovskii, A.; Hummer, G. *Phys. Rev. Lett.* **2002**, *89*, 064503.
(53) Li, J. Y.; Yang, Z. X.; Fang, H. P.; Zhou, R. H.; Tang, X. W. *Chin. Phys. Lett.* **2007**, *24*, 2710−2713.